PERGAMON

Pattern Recognition 36 (2003) 2253–2270

PATTERN RECOGNITION
THE JOURNAL OF THE PATTERN RECOGNITION SOCIETY

www.elsevier.com/locate/patcog

Stability and style-variation modeling for on-line signature verification

Kai Huang*, Hong Yan

School of Electrical and Information Engineering, University of Sydney, Sydney NSW 2006, Australia

Received 18 July 2001; accepted 26 March 2003

Abstract

Stability and style variation are important characteristics in handwriting analysis and recognition. This paper describes a stability modeling technique of handwritings in the context of on-line signature verification. With this technique, the stability and style-variation characteristics of the reference samples are deduced from the dynamic warping relationship between the sequences of basic handwriting strokes. Reliability measures of the extracted signature features are incorporated into the signature segmentation, model building, and verification algorithms, so that stable handwriting features are emphasized in the signature matching process, while style variations for less stable features are intentionally tolerated. The generated signature model consists of a structure description graph of the handwriting components and their stability information. A signature is accepted by the model if it is close to a permissible path within the weighted graph. A novel feature of the technique is its ability to refine the correspondence relation of the handwriting during model building and signature verification. This ability enables the verification and partial correction of segmentation errors to reduce the number of false rejections while maintaining the system security level and keeping the number of reference samples manageable.
© 2003 Pattern Recognition Society. Published by Elsevier Ltd. All rights reserved.

Keywords: Signature verification; Stability; Signature segmentation; Structural description graph

1. Introduction

Signature is a means of personal identity authentication and verification. Its use has been well established in daily activities, especially in legal and commercial environments. For electronic information exchange purposes, it is highly desirable to automate the process of accurately identifying genuine and forged signatures. For this reason, many research efforts have been invested over the last decade [1–3].

Flexible pattern matching techniques are continuously being investigated in solving the signature matching problem, focusing on the temporal and spatial correlation of the signature signals. On-line acquired signature signals, being similar to 1-D speech signals, are distorted by local non-linear expansion and contraction in the temporal domain. Regional correlation, skeleton tree matching [4], elastic matching by dynamic time warping (DTW) [4,5] and signal correlation [6,7], autoregressive modeling [8], hidden Markov modeling (HMM) [9–11], and neural network techniques [12–14] have been applied to this problem with varying degrees of success. Signatures are also 2-D symbols, and non-linear spatial distortion is significant as well [15]. It is customary to examine the finished signature for authenticity rather than the action that produces it. Spatial domain conformance remains as a determining criteria, especially in off-line situations [16–18].

In addition to pattern matching, there are also issues of selecting optimal prototypes and constructing accurate signature models. This is where the analysis of pattern correlation between reference signatures, i.e. stability characteristics extraction, becomes valuable. The aim is to

* Corresponding author. Tel.: +61-2-9351-48-24; fax: +61-29351-3847.

E-mail address: kai@ee.usyd.edu.au (K. Huang).

0031-3203/03/$30.00 © 2003 Pattern Recognition Society. Published by Elsevier Ltd. All rights reserved.
doi:10.1016/S0031-3203(03)00126-2

command an automatic signature verifier to scrutinize the unusual signature style variations, and be less critical on others. The standard deviation is a convenient and generic stability indicator. An alternative stability characteristic for on-line signature verification has been proposed by Dimauro et al., which makes use of the dynamic time warping (DTW) function between the sample points of two signature trajectories [19–21]. In their approach, a direct matching point (DMP) is used to indicate a small region where no significant distortion exists between the trajectories. Stability indices are formulated based on the detection of DMP, and are used to select the optimal reference samples. It seems appropriate to extend their stability estimation method to model handwriting components and strings, i.e. the basic handwriting units as proposed by Plamondon et al. [22–24] over the years. This paper describes such an extension.

In this extended technique, reliable features are identified as those patterns of the handwriting component strings which consistently appear in one's signatures. Matching between signatures is implemented using dynamic warping applied to the respective component strings. Since the dynamic warping algorithm is essentially $O(n^2)$, and the number of handwriting components is much smaller than the number of data samples, performing dynamic warping at the component string level is very efficient. With this technique, the stability characteristics and style variations of the reference signatures are deduced from the warping paths between the sequences of reference components, and are utilized to weight the matching importance of each input and reference component in verification tests. Reliability measures of the extracted features are incorporated into the signature segmentation, model building, and verification algorithms, so that stable handwriting features are emphasized, and style variations at less stable places are intentionally tolerated in the matching process. Signatures are modeled by weighted structure description graph (SDG) of the handwriting components. A signature is accepted by the model if it is close to a permissible path within the weighted graph.

Besides incorporating stability information in the SDG model, another novel feature of this technique is its ability to refine the signature segmentation and the handwriting component correspondence relation. This ability enables the verification and elimination of many signature segmentation errors, and the construction of a more accurate model. As a result, it helps to reduce the number of false rejections while maintaining a high security level.

The paper is organized as follows. Section 2 discusses the extraction of stability characteristics in on-line signatures and the signature model-building process. Section 3 describes the signature verification algorithm which makes use of the stability characteristics in the signature model. The experiment result is presented in Section 4. Finally, the conclusion of this study is given in Section 5.

2. Stability feature extraction

2.1. Signature segmentation

Handwriting-component-based stability measurement requires the signature to be segmented into basic handwriting units. In this instance, segmentation of the on-line acquired signature is performed according to the handwriting motion breaks [25]. It has be observed in the literature that the velocity and curvature changes are closely linked in handwriting trajectories [26], and the pressure waveform varies in synchronization with handwriting motion transitions [27]. The transition points, being near the handwriting velocity zero-crossings, and corresponding to high magnitude local curvature peaks, are chosen as the segmentation points (Fig. 1) [28]. Furthermore, the patterns of these speed-up and slow-down motion transitions are habitually distinct for each writer, and are exploited as a valuable discriminative feature in the on-line signature verification system.

The users of the system are constraint to sign their signatures along predrawn horizontal baselines, similar to those on forms. Horizontal and vertical velocity patterns are used after small angle-range rotation correction of the signature specimen. The rotation angle is estimated by locating the maximum correlation between the direction angle histograms of input and reference template over a small angle range. The initial segmentation is obtained on an individual signature basis (Fig. 2). Over- or under-segmentation, as well as erroneous segmentation, could be expected, due to noise in the data and imperfections of the signature collection process. To construct a more accurate signature model using the limited number of supplied reference samples, a novel segmentation refinement technique is derived, with help from stability measurements, to enhance the signal-to-noise ratio of locating the likely positions of the segmentation points. The segmentation problem can also be reduced by applying model-guided dynamic segmentation techniques [29,30]; however, it is not clear if the stability characteristics are preserved and emphasized by a direct adoption of such approaches.

2.2. Stroke stability estimation

Inspired by the sample-point stability estimation technique by Dimauro et al. [19–21], a method of extracting stability information on handwriting components is implemented. It is based on the analysis of the dynamic coupling between the strings of basic handwriting components in the reference signatures. DTW on basic component strings has its advantages over that on sample points. It evaluates the shape similarity of corresponding handwriting unit as well as the structural similarity of the signature. It preserves component ordering, but also allows limited segment skipping, which is important for modeling style variations. By

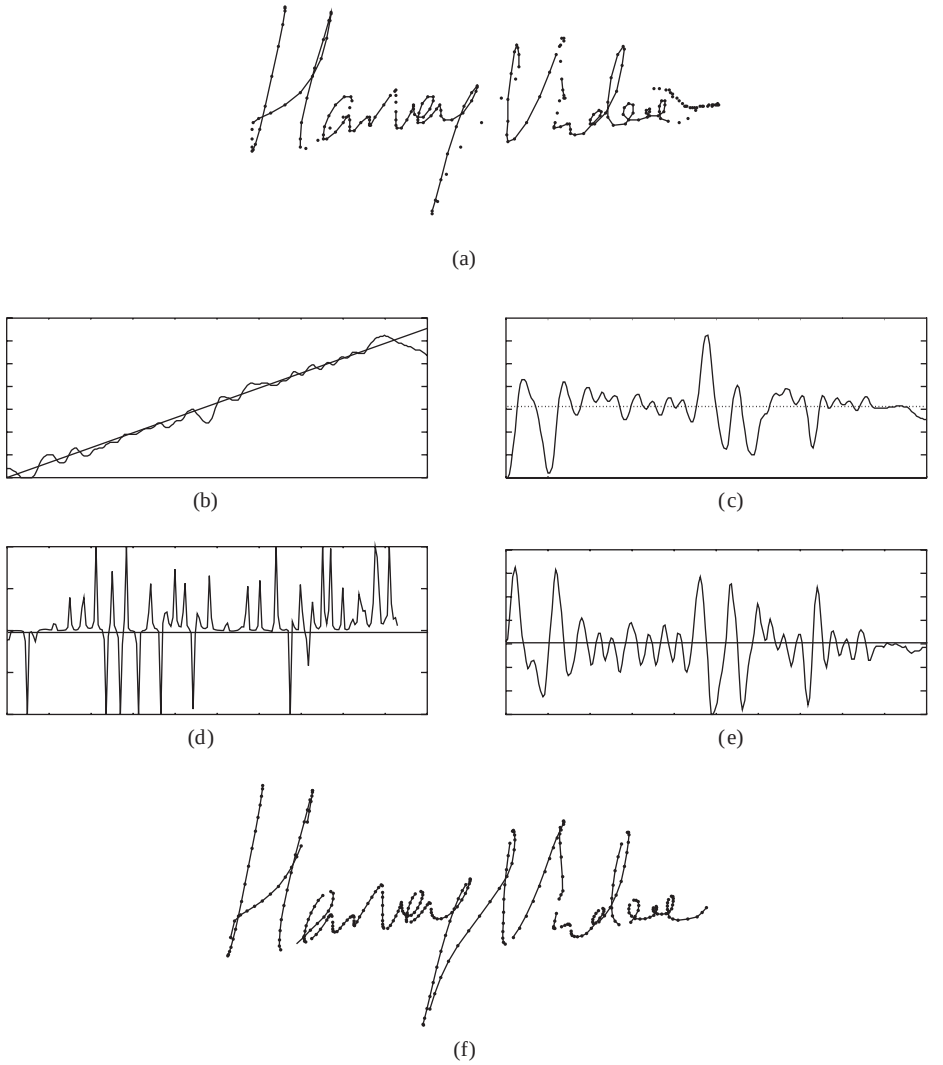

Fig. 1. Illustration of signature functional features and signature segmentation: (a) a signature sample; (b) the function $x(t)$—drifts horizontally; (c) the function $y(t)$—oscillates vertically; (d) the curvature function $\kappa(t)$; (e) the velocity function $v_y(t)$; and (f) the segmented signature trajectory. The zero-crossings of $v_y(t)$ corresponding to a large magnitude $\kappa(t)$ are selected as the signature trajectory segmentation points to obtain the basic handwriting units.

imposing intermediate structural boundaries and hence semantics information in the matching process, it improves upon the sample-point dynamic warping in reducing the matching errors.

For a set of genuine reference samples $R=\{S^i|i=1,\ldots,n\}$, the stability of a single specimen $S^r \in R$ is formulated with respect to the other signatures $S^v \in R$, $r \neq v$. Assume a signature is represented as a list of segmented basic handwriting units, i.e.,

$$S^r = s_r(1) + \cdots + s_r(p) + \cdots + s_r(n_r),$$

$$S^v = s_v(1) + \cdots + s_v(q) + \cdots + s_v(n_v), \quad (1)$$

where $s_r(p)$ and $s_v(q)$ are the basic units of corresponding signatures as identified by the signature segmentation method, and n_r and n_v are the numbers of such units within the signatures (Fig. 2).

The dynamic warping procedure generates the coupling sequence, $W(r,v)=(i_1,j_1),\ldots,(i_k,j_k),\ldots,(i_K,j_K)$, of length K, between the basic units of S^r and S^v. (i_k,j_k) denotes a coupling between $s_r(i_k)$ and $s_v(j_k)$, $1 \leqslant i_k \leqslant n_r, 1 \leqslant j_k \leqslant n_v$. The accumulated global distance,

$$D(S^r,S^v) = \sum_{k=1}^{K} d(s_r(i_k), s_v(j_k)), \quad (2)$$

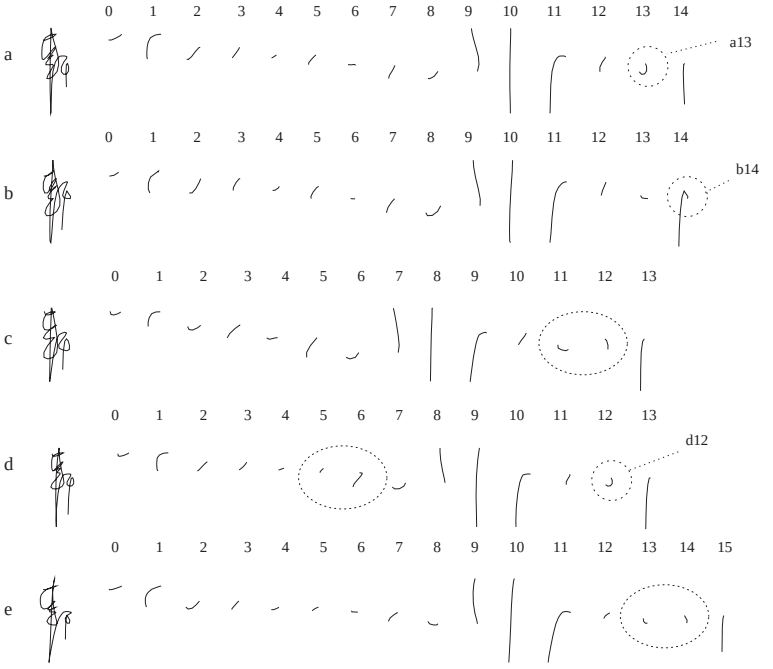

Fig. 2. A set of reference signatures from the database and their respective segment sequences are shown. It is used as an example in the description of the signature model-building algorithm. It can be observed that some segments, e.g. a13, d12, and b14, are not segmented completely. These will either be corrected by the segmentation refinement algorithm or go undetected causing matching problems.

is to be minimized by the warping algorithm, where $d(s_r(i_k), s_v(j_k))$ is the component stroke distance (to be defined in Section 3) between the basic units of S^r and S^v (Fig. 3).

The multiplicity of the coupling relation of a handwriting component is defined as the number of consecutive occurrences of the component index which appear in the warping path $W(r,v)$, where the consecutive property is implied by the use of the DTW algorithm. Let $(p,q) \in W(r,v)$ be an identified coupling between components $s_r(p)$ and $s_v(q)$, where p and q are the indices of the matching components, respectively. The multiplicities m_p and m_q are given as

$$m_p = card\{(i_k, j_k) \in W(r,v) \mid i_k = p\},$$

$$m_q = card\{(i_k, j_k) \in W(r,v) \mid j_k = q\}, \tag{3}$$

where $card\{.\}$ gives the cardinality of a set.

A direct matching segment (DMS) of the rth signature is a pen-stroke segment which has a one-to-one coupling with a pen-stroke segment of the vth signature, i.e. the multiplicities of the components in the coupled pair are both 1:

$$s_r(p) \text{ is a DMS } \Leftrightarrow m_p = m_q = 1. \tag{4}$$

For each component of the rth signature, a value indicating the goodness of match under dynamic warping can be assigned according to its coupling with components of the vth signature. A decision scheme for assigning such a value is given as

$$C(S^v(s_r(p))) = (\tfrac{1}{2})^{m_p + m_q - 2}, \quad \forall p \in \{1, \ldots, n_r\}, \tag{5}$$

where m_p and m_q are the multiplicities of the coupling components.

The index of local component stroke stability for the rth signature with respect to the reference set R is given by the columnwise average, i.e., for the case $S^r \notin R$,

$$I(s_r(p)) = \frac{1}{n} \sum_{v=1}^{n} C(S^v(s_r(p))), \quad p = 1, 2, \ldots, n_r, \tag{6}$$

and for $S^r \in R$,

$$I(s_r(p)) = \frac{1}{n-1} \sum_{v=1, v \neq r}^{n} C(S^v(s_r(p))),$$

$$p = 1, 2, \ldots, n_r, \tag{7}$$

which is the stability index formulation of the leave-one-out training procedure.

In the example of Fig. 3, the detected DMS sequence value of signature S^r is

$\{1,1,1,1,1,1,1,1,1,1,1,1,1,1,1,1\}$,

$\{1,1,1,1,\tfrac{1}{4},\tfrac{1}{4},\tfrac{1}{4},1,1,1,1,1,1,\tfrac{1}{2},1\}$,

$\{1,1,1,1,1,\tfrac{1}{4},\tfrac{1}{4},\tfrac{1}{8},1,1,1,1,1,1,1\}$,

$\{1,1,1,1,1,1,1,1,1,1,1,1,\tfrac{1}{2},1,1\}$.

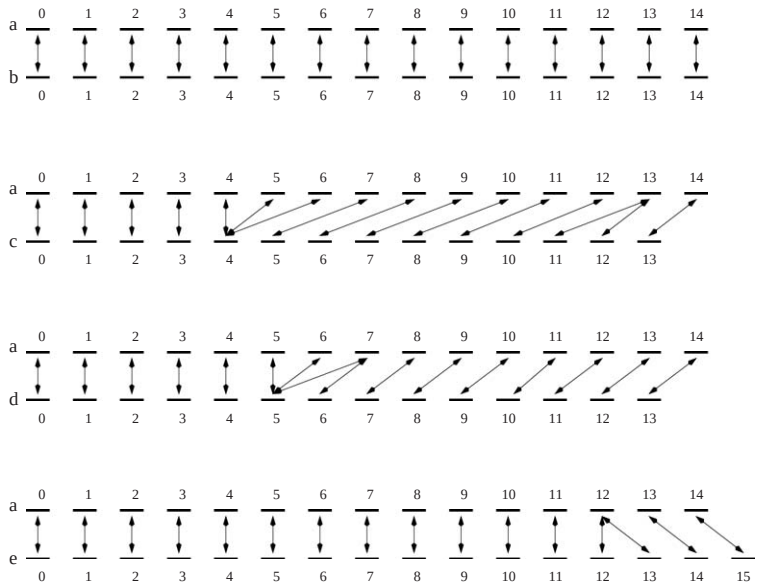

Fig. 3. Illustration of the handwriting stroke segment warping relation in the set of five reference signatures in Fig. 2. The sequence of handwriting components of a signature S^r denoted by a is matched against other reference signatures (b–e). These warping relations are processed by the subsequent segmentation refinement and model-building steps to derive stability features within a signature.

The local stability indices of the individual components of S^r are

$$\{1, 1, 1, 1, \tfrac{26}{32}, \tfrac{20}{32}, \tfrac{20}{32}, \tfrac{25}{32}, 1, 1, 1, 1, \tfrac{28}{32}, \tfrac{28}{32}, 1\}.$$

The stable-coupling chains, i.e. the strings of uninterrupted DMS coupling indicated by continuous strings of 1s, give useful indications of long component string stability. Stability index of pen-stroke sub-groups is generally given as

$$I(s_r(p), w) = \frac{1}{card(V)} \sum_{p' \in V} I(s_r(p')),$$

$$p = 1, 2, \ldots, n_r, \tag{8}$$

where $V = \{p' : 1 \leqslant p' \leqslant n_r, |p' - p| \leqslant w\}$ and $card(V)$ gives the number of elements in set V. By adjusting the neighborhood size w hence the neighborhood set V, the stability indices of component stroke combinations are obtained. Since the handwriting components are the basic matching units in this case, typically, w is assigned values of 1, 2, and 3, to generate the corresponding levels of component sub-group stability indices. When $w = 1$, the indices of the immediate previous and next neighbors of a segment in the component string are included in the evaluation of Eq. (8). The range is three consecutive components. Similarly, when $w = 2, 3$, five and seven consecutive components are considered. The decision values for component indices outside the physical range are assumed to be 0.5, to reduce edge effects, for the purpose of calculating the long-range stability values. The local stability indices for individual components can be regarded as a special case for which $w = 0$. This multi-level neighborhood modeling scheme encompasses the local to long-range stable stroke-segment coupling stability confidences, as shown in Fig. 4. The detection of peak values at each level produces the location and range of the consecutive stable components.

The medium-to-large amplitude velocity variation pattern of stable pen-movement components is very interesting. It is characterized in the vertical or horizontal velocity timing diagram as several bursts of highly active peak/trough variations, which are also evident in carelessly signed signatures (Fig. 5). They represent highly skilled groups of handwriting sub-strokes which can be expected to be present in most, if not all, genuine signatures. The ranges of such stable coupling of stroke sub-groups, referred to as the velocity-activity groups, are recorded in the corresponding signature model, via sub-group stability indices $I(s_r(p), w)$ being approximately equal to 1, for each level of w. The corresponding functional features in the detected ranges at each level are used in verifying the existence and similarity of such activity groups in an input signature.

In the following sections, the identified DMS and non-DMS couplings (Fig. 6) are utilized in the construction and refinement of the signature model.

2.3. Structural model building

SDG is a visually appealing scheme for organizing the complex statistical features and structural relations in on-line acquired signatures. Dimauro et al. [31,32] have utilized it to model handwriting strokes separated by pen-lifts, by

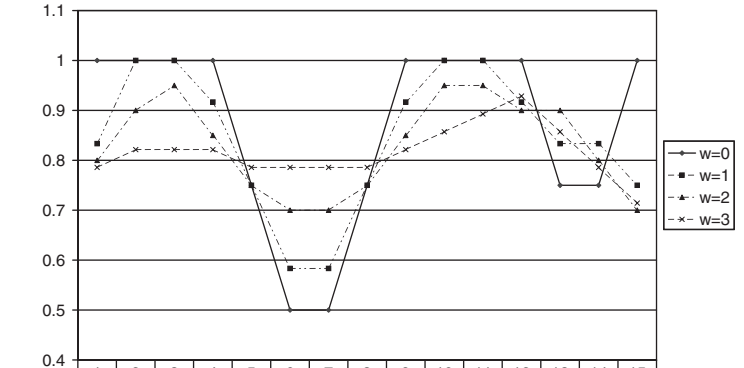

	1	2	3	4	5	6	7	8	9	10	11	12	13	14	15
w=0	1	1	1	1	0.75	0.5	0.5	0.75	1	1	1	1	0.75	0.75	1
w=1	0.83	1	1	0.92	0.75	0.58	0.58	0.75	0.92	1	1	0.92	0.83	0.83	0.75
w=2	0.8	0.9	0.95	0.85	0.75	0.7	0.7	0.75	0.85	0.95	0.95	0.9	0.9	0.8	0.7
w=3	0.79	0.82	0.82	0.82	0.79	0.79	0.79	0.79	0.82	0.86	0.89	0.93	0.86	0.79	0.71

Fig. 4. Multi-level neighborhood stability indices.

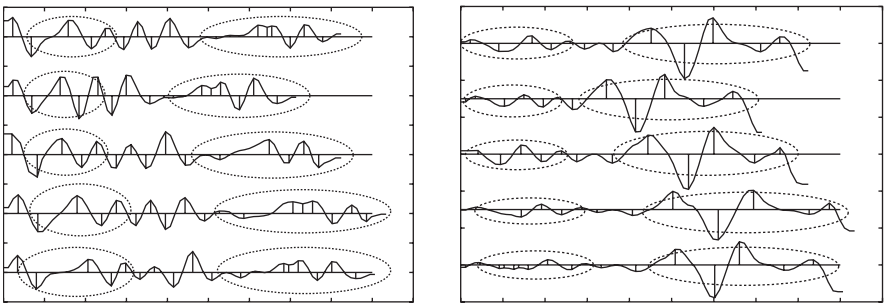

Fig. 5. An illustration of the velocity variation pattern within a set of reference signatures, showing (a) horizontal velocity pattern $v_x(t)$ and (b) vertical velocity pattern $v_y(t)$. The dashed-line enclosed regions correspond roughly to the stable DMS sub-groups which are characteristic in the signature, referred to as the velocity-activity groups.

identifying the finite set of pen-lift singularity positions within the reference samples, and using an improved k-means clustering technique to group the handwriting strokes into fundamental stroke component clusters via topological features and the point-ordering information in the signature. Similarly, SDG is used here to describe the organization of the motion-segmented handwriting components obtained in Section 2.1, where there are typically several basic handwriting units within a single pen-lift separated stroke. For each enrolled signature, an SDG is constructed by identifying the finite set of handwriting component clusters from the reference samples via dynamic warping of the component strings.

The dynamic warping sequences are algorithmically transformed into an SDG (Fig. 7). In the transformation, the components in the template signature are treated as initial cluster centers. The components in the other reference signatures under DMS coupling are grouped directly with these centers (Fig. 7a). The non-DMS coupled components are extrapolated as branches from the main trunk, which then become separate clusters. The branch returns to the main trunk when DMS coupling resumes. The stability values associated with these clusters are the ratio of the numbers of components in the clusters over the number of total reference signatures. The uninterrupted DMS coupling sequences are also well presented in the SDG, as the concatenation of consecutive main trunk components without any branches.

The internal algorithmic implementation of the SDG is illustrated in Fig. 8. On the main trunk of the directed graph data structure, there are a number of conceptual nodes which separates the handwriting components. The components are represented as the directed links between the nodes. Each node maintains lists of branch-in and branch-out

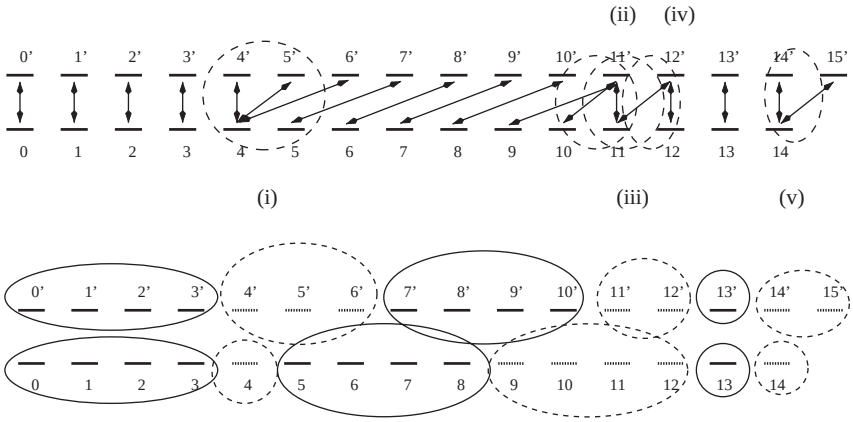

Fig. 6. Identifiable stability patterns within the dynamic warping output. The stable DMS-coupling patterns, i.e. the one-to-one relations, are circled with solid lines. The non-DMS-coupling patterns, i.e. one-to-many relations, are circled with dotted lines. Non-DMS patterns may appear in many forms. For example, in case (i), it is located in the middle of the component sequence; in cases (ii)–(iv), it spans more than one node; and in case (v) it is located at one end.

pointers. Branches originate from the nodes where a transition from DMS to non-DMS occurs, and terminate in subsequent nodes where DMS matching resumes. Each link or branch has a list of attributes, which includes the starting and finishing node numbers and the references to the originating stroke and signature.

Let A_i be any stroke-segment cluster on the SDG main trunk of reference signature S^r. If the number of components in A_i is greater than one, a set of verification thresholds $\theta(A_i)$ will be calculated to represent the extents of the feature variations within this cluster. For clusters on the SDG branches, cross-references are created via pointer links to other SDGs where these branch clusters are on the main trunk in their respective SDGs.

The obtained SDG is only an initial but a useful estimate of the signature model. This is because the DTW procedure is an optimization procedure, not a clustering procedure. Errors in the matching pairs mainly exist for the non-DMS coupling regions. For example, in Fig. 7(b), 11c+12c correctly matches to a13, but 12e+13e should not be matched to a12. A segmentation verification and refinement process is necessary to rectify these errors.

2.4. Segmentation verification and refinement

The non-DMS patterns as identified by the analysis of handwriting component warping are further analyzed together with their neighboring components by a segmentation verification process, to decide on how the components can be best correlated. Consider the typical non-DMS coupling examples in Fig. 6, in which there are a few possibilities. First, it is possible that the segment may simply need to be repeated several times as detected by the dynamic warping algorithm. It is also possible that over- or under-segmentation for one of the signatures occurs. The neighboring components of the excessively segmented region need to be combined before matching to the corresponding region. Finally, the regions under comparison may differ sufficiently so that after eliminating the possibility of shorter range coupling, a combined long segment in one signature has to be matched with a combined long segment in another signature.

Non-DMS coupling patterns can generally appear in the forms listed in Fig. 9. Let $b(y_1, y_2, \ldots, y_n)$ denote all the possible configurations that can be generated for the one-to-many relation $b \rightarrow (y_1, y_2, \ldots, y_n)$. In the following, '$\rightarrow$' denotes 'is matched to', and '$+$' denotes 'is concatenated with'. For $n = 1$, $b(y_1)$ is simply $b \rightarrow y_1$. For $n = 2$, $b(y_1, y_2)$ represents the following two configurations: $\{b \rightarrow y_1, b \rightarrow y_2\}$; and $\{b \rightarrow y_1 + y_2\}$. Configurations for higher orders of n are generated recursively by expressions involving lower-order terms. For example, $b(y_1, y_2, y_3)$ is equivalent to $\{b \rightarrow y_1, b(y_2, y_3)\}$; $\{b \rightarrow y_1 + y_2, b(y_3)\}$; and $\{b \rightarrow y_1 + y_2 + y_3\}$. The general case $b(y_1, y_2, y_3, \ldots, y_n)$ represents $\{b \rightarrow y_1, b(y_2, y_3, \ldots, y_n)\}$; $\{b \rightarrow y_1 + y_2, b(y3, \ldots, y_n)\}$; …; and $\{b \rightarrow y_1 + y_2 + \cdots + y_n\}$.

The rules of generating the configurations for case (a) of Fig. 9 are:

- $a \rightarrow u,\ b(y_1, y_2, \ldots, y_n),\ c \rightarrow v$;
- $a \rightarrow u + y_1,\ b(y_2, \ldots, y_n),\ c \rightarrow v$;
- $a \rightarrow u + y_1,\ b(y_2, \ldots, y_{n-1}),\ c \rightarrow y_n + v$;
- $a \rightarrow u,\ b(y_1, y_2, \ldots, y_{n-1}),\ c \rightarrow y_n + v$.

In case (b) of Fig. 9, they become:

- $a \rightarrow u,\ b(y_1, y_2, \ldots, y_n),\ c \rightarrow v$;
- $a \rightarrow u + y_1,\ b(y_2, \ldots, y_n),\ c \rightarrow v$;

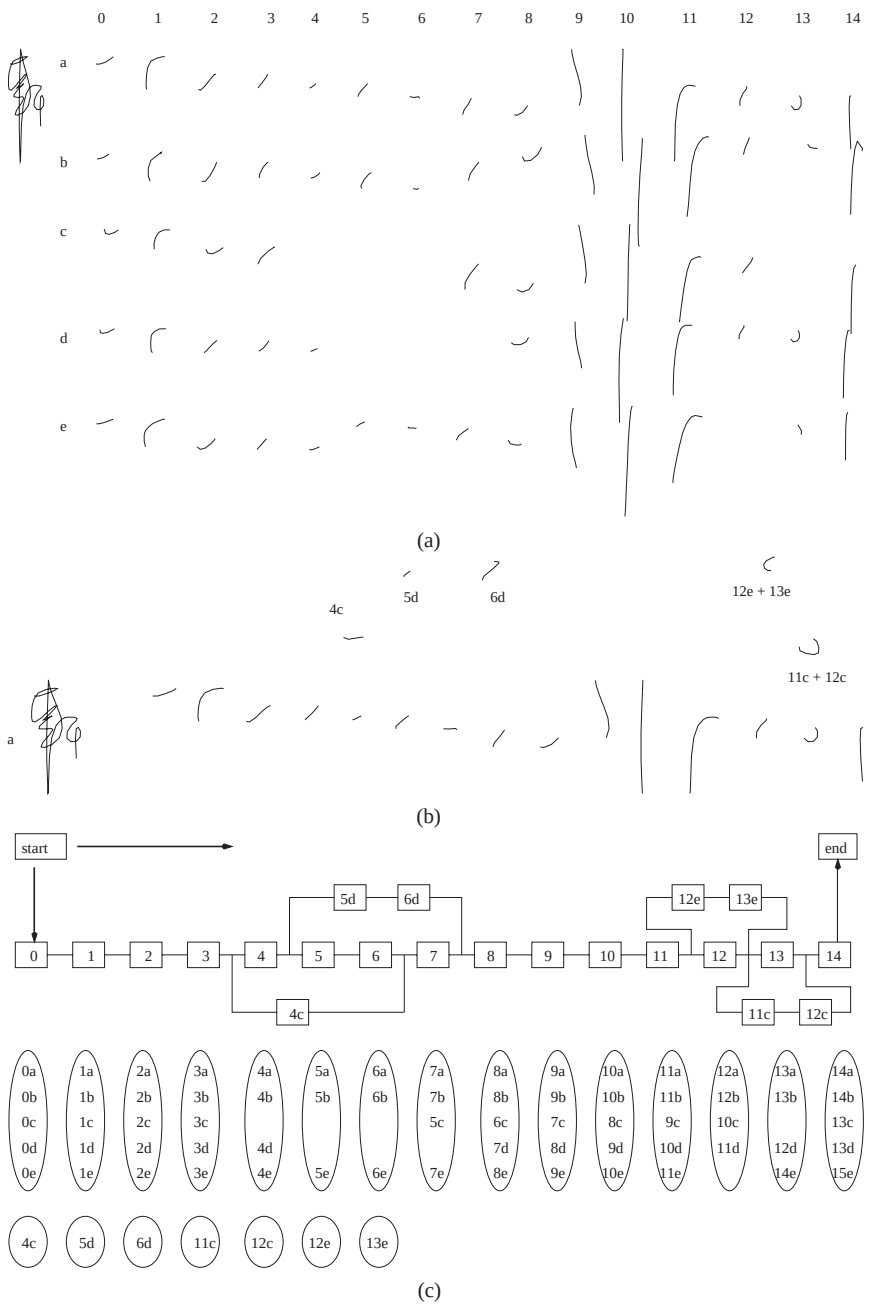

Fig. 7. The SDG of a signature model. Each ellipse enclosed group is a component cluster. (a) component clusters as identified by DMS couplings, (b) non-DMS components, and (c) a conceptual diagram of SDG for a reference signature.

- $a \rightarrow u + y_1,\ b(y_2, \ldots, y_n, v),\ c \rightarrow v$;
- $a \rightarrow u,\ b(y_1, y_2, \ldots, y_n, v),\ c \rightarrow v$.

The $a \rightarrow u$ and $c \rightarrow v$ couplings may not always be present. This happens when the one-to-many relation is at one end of the component string, in which case these terms are discarded in the list of rules. The distances at sample point level of the possible configurations in these cases are evaluated, and the likelihood of the configurations are ranked accordingly. In the cluster refinement step, the most likely configuration is chosen to be the correct component coupling relation, and the model graph is adjusted accordingly so that uncertainties in the initial SDG are removed. An example on model refinement is given in Fig. 10. The algorithm of

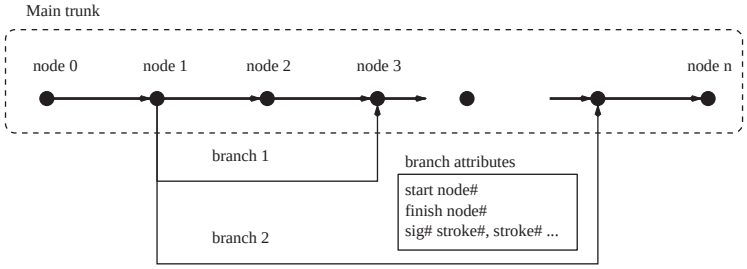

Fig. 8. SDG in the form of a directed graph.

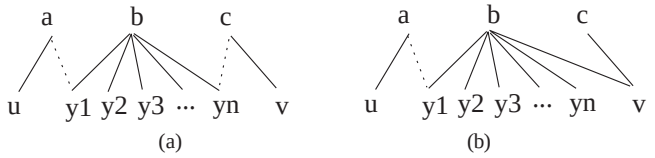

Fig. 9. General case of non-DMS coupling from component-warping. Stroke b is the non-DMS coupling under consideration. Case (a) is a simple one-to-many matching enclosed by DMS couplings at both ends and case (b) is a many-to-many matching due to an extra link between b and v. The solid lines indicate the actual matching pairs under dynamic warping. The dotted lines indicate other permissible matchings.

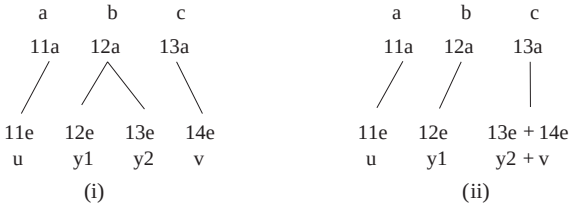

Fig. 10. An example of SDG model refinement: (i) the initial model configuration as dictated by dynamic warping algorithm and (ii) the updated model configuration after applying the rules of Fig. 9(a). The last rule of case (a) applies.

component stroke clustering and refinement is summarized below.

Algorithm of component match refinement

- For signature $S^r \in R$, obtain the component coupling sequences $W(r,v)$, $\forall S^v \in R,\ v \neq r$, with dynamic warping.
- From each $W(r,v)$, calculate the multiplicities of stroke components in S^r and S^v according to Eq. (3), and identify the DMS and non-DMS in the sequence. The component whose multiplicity $m = 1$ is a DMS, otherwise it is a non-DMS.
- For each non-DMS region, perform the following segmentation verification procedure.
  - Derive the possible segment configurations according to rule set for cases (a) and (b) in Fig. 9, and calculate their matching distances.
  - Select the most likely configuration according to the least distance.
- Re-calculate the stability indices of the signature components, using the updated configuration, and re-generate the SDG model from the refined coupling.

After segmentation verification and refinement, the SDG model of Fig. 7 becomes Fig. 11. Referring to Figs. 2 and 11, it can be seen that the branch 4c models the situation of missing components in signature c; and the branches 5d+6d, 11c+12c and 13e+14e model the situations of component style variation or incomplete segmentation of the signature d and the model signature a, respectively. In this particular SDG model, component cluster 13a is updated to include the combined long components 11c+12c and 13e+14e, and it is relabeled as a probable DMS region after the refinement process.

3. Signature verification

The online signature verification algorithm adopts a multi-stage strategy. Global features, such as the aspect ratio, the signature length and time duration, average and maximum speed, and the 2-D bitmap features, are used to filter the random and less skillful signature forgeries [28,33]. While establishing the correspondence of handwriting components by the dynamic warping procedure, the presence and absence of the reference components are examined, i.e. a structural feature verification is performed. The functional feature distances, between the input signature and the model, over each matched component stroke pairs and the long-range stable velocity-activity groups, are then accumulated and combined to generate an overall matching score.

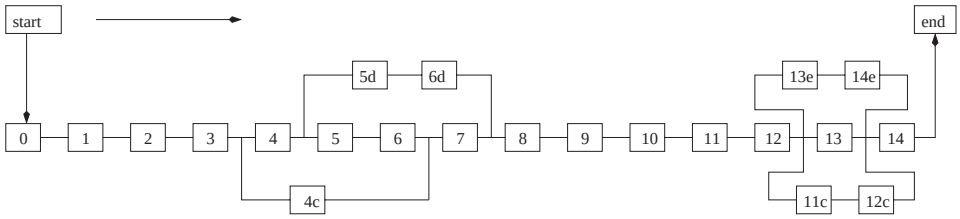

Fig. 11. A refined SDG model. It shows that the concatenation of the 13th and 14th segment of signature e (13e+14e) corresponds to the template segment 13a, which differs from the initial model shown in Fig. 7(c).

3.1. Stroke distance metrics

The functional distance of shape change between corresponding signature components is computed with the aid of B-spline approximation, adopting the curve distance metrics formulated in a previous work [34]. This approximation gives analytical solution to the first and second derivatives of the curve, and the matching distance is a shape-feature-based one. However, because it operates only on the segmented signature components, the loss of dynamical handwriting information is also minimized.

Let $s_r(p)$ be a model handwriting component curve of n equidistance points, and $s_v(q)$ a corresponding component curve in the test pattern. $s_v(q)$ is reconstructed from its B-spline representation to be of the same dimension n. The shape change between these curves, $d(s_r(p), s_v(q))$, is defined to be a measurement of the elastic deformation in transforming from $s_r(p)$ to $s_v(q)$, where the Euclidean distance term E_d, the strain energy term S_e, and the bending energy term B_e are given by

$$E_d[l] = \| s_r(p)[l] - s_v(q)[l] \|^2,$$

$$B_e[l] = \left\| \frac{\mathrm{d}^2 s_r(p)[l]}{\mathrm{d}s^2} - \frac{\mathrm{d}^2 s_v(q)[l]}{\mathrm{d}s^2} \right\|^2,$$

$$S_e[l] = \left\| \frac{\mathrm{d}s_r(p)[l]}{\mathrm{d}s} - \frac{\mathrm{d}s_v(q)[l]}{\mathrm{d}s} \right\|^2, \tag{9}$$

where $\|.\|$ indicates the Euclidean norm of a vector.

Let $d[l]$ be the pointwise distance between corresponding samples on $s_r(p)$ and $s_v(q)$:

$$d[l] = \sqrt{\alpha E_d[l] + \beta S_e[l] + \gamma B_e[l]}, \tag{10}$$

where α, β and γ are weighting constants denoting the contributions of the distance components, with $\alpha + \beta + \gamma = 1$. The total distance of stroke component shape variation is

$$d(s_r(p), s_v(q)) = \sum_{l=1}^{n} d[l]. \tag{11}$$

The functional feature distances of pattern variations about pen-movement direction, velocity, acceleration, and pressure and pen-tilt angles when available, between corresponding handwriting stroke components, are computed with the aid of DTW on the respective component pairs.

3.2. Verification algorithm

The block diagram of the detailed signature verifier is given in Fig. 12. For each signature category enrolled, five reference signatures are used by default to construct the corresponding statistical verification model. In principle, the verification process operates by rectifying the errors in signature segmentation and refining the stroke-correspondence mapping in order to obtain an accurate model. An SDG is built for each reference signature and the collection of all the reference signature SDGs is the signature model. During model building, each of the reference signatures in turn is used as a test input, to generate a set of acceptance thresholds for each handwriting component cluster and the identified velocity-activity groups within the model. In the verification phase, an input signature is tested against the SDG models. Utilizing the cluster thresholds, the lists of accepted and rejected input components, as well as the omitted reference components, are generated. The final decision is based on the analysis of these lists, as well as the matching results on the functional features of long-range velocity-activity groups.

The input signature is accepted by the signature model if there exists a path within an SDG which is sufficiently similar to the input sequence. The test for such a condition is implemented with a straightforward strategy, i.e. to generate all the permissible paths within the SDG, and comparing each path against the input sequence. A more efficient strategy is to perform the dynamic warping and refinement procedure between the SDG main trunk and the input component sequence, and then to consider localized matching with the SDG branches for non-DMS coupled input components. The former strategy is described and used here for its simplicity. The implementation of the latter strategy is being verified at this stage. The accuracy of the end result however is not dependent on which of the two strategies used.

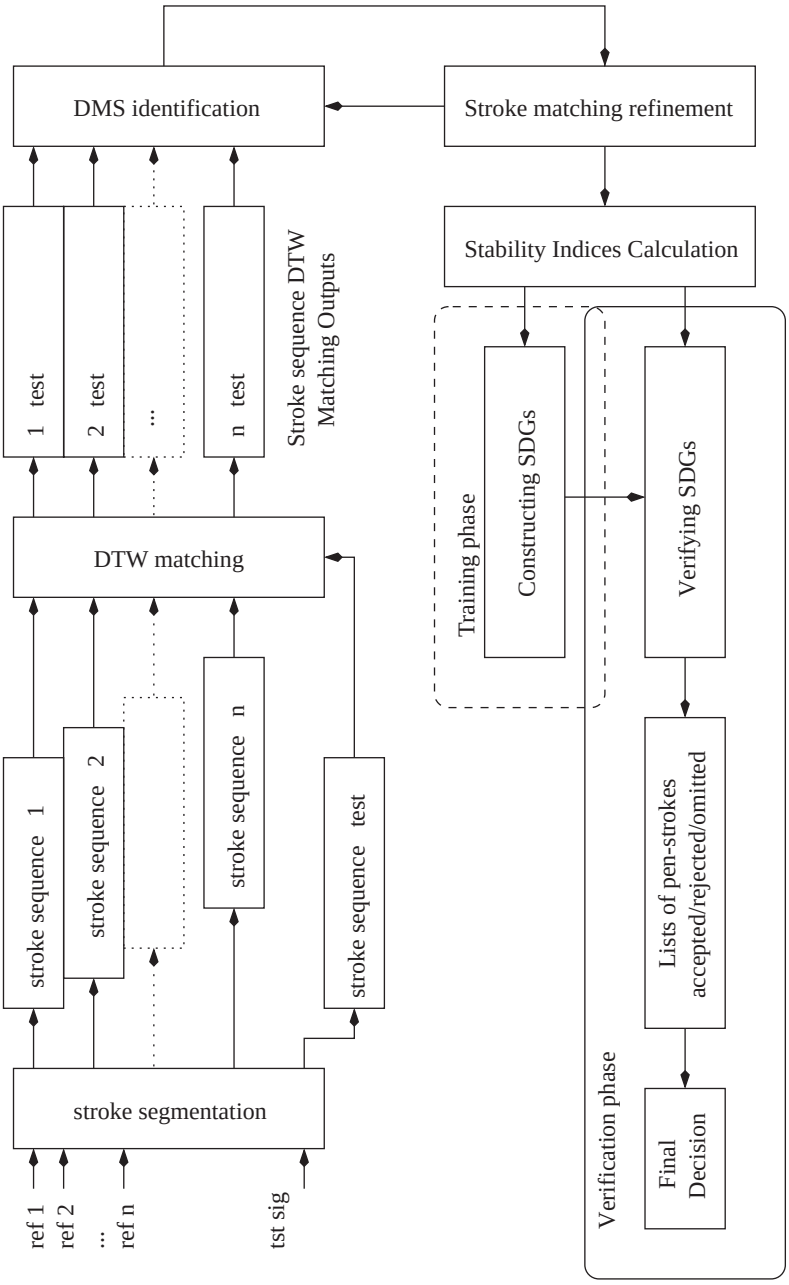

Fig. 12. The block diagram of the detailed signature verifier of the on-line signature verification system implemented.

Algorithm of model acceptance testing

- For each SDG^i, $i \in [1..n]$ in the signature model, create an initial path p_j^i, with $j = 0$, and generate all permissible paths
- GenPath(p_j^i, j)
  - Add links to path p_j^i along SDG^i, till the end node is reached or a node with branches is encountered.
  - If the end node of SDG^i is reached, return p_j^i.
  - If encountering a node with branch-outs, create a temporary $p_t = p_j^i$:
    for each branch-out {
    create a new path p_{j+1}^i;
    copy p_t to p_{j+1}^i;
    recursively call GenPath($p_{j+1}^i, j+1$);
    }

- For each path $p_j^i = s_1^i + \cdots + s_r^i + \cdots + s_{k_r}^i$, obtain the distance to the input signature component path $t = s_1 + \cdots + s_t + \cdots + s_{k_t}$:
  - Perform stroke-match to obtain the warping sequence $W(p_j^i, t)$.
  - Perform cluster membership test on the input components along $W(p_j^i, t)$.
  - Accumulate the lists of accepted, rejected input components, and the omitted reference components.
  - Accumulate the weighted global distance d_{total} for path p_j^i.
- Make a final decision on the acceptance of input signature t, based on a list of criteria.

The weight of each template component s_r^i in p_j^i is calculated by taking into account its length as well as its stability index:

$$weight(s_r^i) = \frac{length(s_r^i) \times I(s_r^i)}{\sum_{l=1}^{k_r} length(s_l^i) \times I(s_l^i)}. \tag{12}$$

The total weighted distance of input signature against reference model is

$$d_{total} = \sum_{l=0}^{K} weight(s_{w_1}^i) \times d(s_{w_1}^i, s_{w_2}), \tag{13}$$

where $(w_1, w_2) = W(p_j^i, t)(l)$.

The weight of each input component s_t is the component length over the sum of lengths of all input components, assuming they are equally stable:

$$weight(s_t) = \frac{length(s_t)}{\sum_{l=1}^{k_t} length(s_l)}. \tag{14}$$

Assume a pen-stroke component s_t of input signature t has a matching reference component s_r^i of p_j^i in the warping sequence $W(p_j^i, t)$. s_t is accepted by the s_r^i cluster if the deviations of its feature values are within the model cluster thresholds. Otherwise it is either rejected, if the reference component s_r^i is a DMS, or marked as a style variation in which case the deviation is accumulated in the global distance. In the case that s_t is rejected, s_r^i is marked as an omitted component by t. Statistical data are also recorded on whether the uninterrupted chains of DMS in p_j^i has been broken.

Judgement of whether the input signature is acceptable to the signature model is based on the following criteria, by comparing to the corresponding statistics obtained from the reference signatures:

- the accumulated weights of accepted components of t by p_j^i, $Acc(p_j^i, t)$;
- the accumulated weights of rejected components of t by p_j^i, $Rej(p_j^i, t)$;
- the accumulated weights of omitted components of p_j^i by t, $Omt(p_j^i, t)$;
- the accumulated weighted distance d_{total} for each p_j^i;
- the conformance of stable DMS sequences within p_j^i by t.

3.3. Verification confidence value generation

There are T security levels defined in the implemented signature verification system, where $T = 10$ by default. Let N be the number of verification tests to be performed. In each verification test, whether it is on global parameters or local component statistics, let δ_i be the standard deviation of the feature value computed from the reference signatures. The minimum and maximum threshold values correspond to δ_i and $5\delta_i$, respectively. The range of each confirmation test thresholds (between minimum and maximum) is evenly divided into steps according to the number of security levels, with smaller threshold values corresponding to higher security levels. If the conformation tests are passed for all security levels upto t_i, but failed at the more strict level t_i, where $0 \leqslant t_i < T$, and only $N_p(t_i) < N$ tests are passed, the confidence score h is

$$h = \left(t_i + \frac{N_p(t_i)}{N}\right) \times \frac{100\%}{T}. \tag{15}$$

The verification tests are arranged so that global parameter tests are performed first, and if these fail, the detailed local component tests are skipped by assuming they also fail. A weighting factor may be assigned for each test, to indicate its relative importance in all the N tests. Here it is assumed they are equally important.

4. Experiment results

4.1. Signature data

At first, a Summagraphics tablet is used to collect on-line signature data. It is equipped with a 6×6-in^2 opaque writing area, a wired pen, and a pen-down/pen-up switch operated by the pen-tip touching the writing surface. It is set at a resolution of 500 lines/in, and a report rate of 50 coordinate pairs/s for the experiment. A Wacom Intuos 4×5-in^2 tablet with a cordless pen is also used. It provides a higher relative resolution of upto 2540 lines/in, a higher sampling rate of upto 200 coordinate pairs/s, and pen-pressure information quantized to a 10-bit dynamic range. The Intuos pen also reports the pen tilt angle to 1° relative accuracy. Both hardware settings are capable of capturing the pen-tip position in the proximity of the flat tablet surface. The pen trajectory is displayed on a nearby computer monitor as the signature signing takes place. On the monitor, pen-down traces are displayed as solid lines, and pen-up traces as light, dotted lines. An IBM CrossPad tablet is also used briefly in a trial. The data quality is comparable to that from the Wacom tablet, and users generally find it more comfortable to write on with its paper and ink interface.

The signature data are collected at various stages of the experiment. The total number of on-line handwriting samples collected from various persons, including targeted forgery signatures, is about 4600, belonging to 89 classes, with about

Table 1
Table showing the composition of collected on-line signature/handwriting data during the experiment

Database	Tablet	ID range	Content	Total classes
DB1	Summagraphics	00–25	Practiced names	26
DB1	Summagraphics	26–48	Signatures	23
DB2	Wacom Intuos	49–68	Signatures (English)	20
DB2	Wacom Intuos	69–84	Signatures (Chinese)	16
DB2	IBM CrossPad	85–88	Signatures (English)	4

2100 belonging to the 36 classes obtained using the Wacom Intuos tablet, 160 belonging to the 4 classes from IBM CrossPad, and the rest obtained using the Summagraphics tablet. Each writer contributes about 20 genuine signatures, and various number of targeted forgery signatures. The number of forgery signatures for each class is approximately the same, which is about 30. The database is divided into sub-groups DB1 and DB2 as shown in Table 1, while performing global random forgery test analysis. Targeted forgery detection is emphasized in the tests. The final test results are obtained for the complete set of data, i.e. DB1 and DB2 combined.

4.2. Classification using global parameters

Global parameters tests on data collected from the Summagraphics tablet (Data set DB1) and the Wacom tablet (Data set DB2) are given in Fig. 13. These tests involve examining the parameter features extracted within non-overlapping rectangular grids of the distribution of sample points, high curvature regions, and the direction of pen-movements, as well as the number of sub-strokes, total signing duration features. Generally speaking, the global test results of the two data sets follow similar patterns, in that the FRR curves and the FAR curves on targeted forgery signatures show much resemblance. The curves on random forgery tests are different, in that the FAR value for DB1 is higher.

In the current form of the algorithm, higher temporal sampling rates than 50 Hz does not significantly improve the signature segmentation and matching accuracy. However, the higher spatial sampling resolution offered by the tablets for constructing DB2 does seem to make a difference in rejecting random forgery signatures, in that the FAR of DB2 on random forgery data is lower than that of DB1. The inclusion of practiced names in DB1 also contributes to a higher FAR because a practiced name is not as stable as a normal signature.

5. Targeted forgery signature tests

The pressure information reported by the Wacom tablet proves to be valuable in preprocessing and signature segmentation. In the preprocessing stage, most spurious and unintentional pen-down sample data can be identified by their close to zero pressure reading and are removed. The pressure information also gives valuable hints on where the handwriting motion tends to break. By combining the evidences in handwriting pressure reaching a local minimum with the vertical or horizontal pen-velocity reaching a zero-crossing and the curvature value approaching a local peak, the correctness of a signature segmentation decision is improved.

Pressure information adds a new dimension to on-line signature verification. Shape, velocity, and pressure patterns are a powerful combination in detecting forgery signatures. Applying pressure information in the local elastic matching stage works quite well for a number of signatures; however, it also increases the false rejection of others. From observations, the pressure-waveforms are not always as stable as the position- and velocity-waveforms for the data sets in this experiment, and because not all signature data contain pressure information, they are not used during detailed signature feature verification, but are used during preprocessing and segmentation. The writer may need a few practices to get familiar with the feel of the data capturing device and therefore the first few samples usually exhibits inconsistency in the handwriting waveforms. This is also reported by Bromley et al. [12]. For each subsequent data capture session, the writer needs to re-adjust him- or herself from the use of normal pen, especially when distracted by looking at the computer monitor for visual feedback. An integrated tablet and LCD display may be the answer to capture more consistent on-line signature data.

The application of SDG stability modeling is effective in the experiment. All the data from DB1 and DB2 are used in the test. The first five samples of each enrolled signature class are used to build the reference model, and the rest signatures are used as test samples.

The on-line signature verification algorithm is tested on the experimental database, using the first five reference signatures in each signature class to build the signature model. Varying the number of reference signatures between five to eight gives slight but steady performance improvements in the error trade-off curves. However, the more the reference signatures used, the more strict the verification thresholds needed. If less reference signatures are used, e.g. three, the

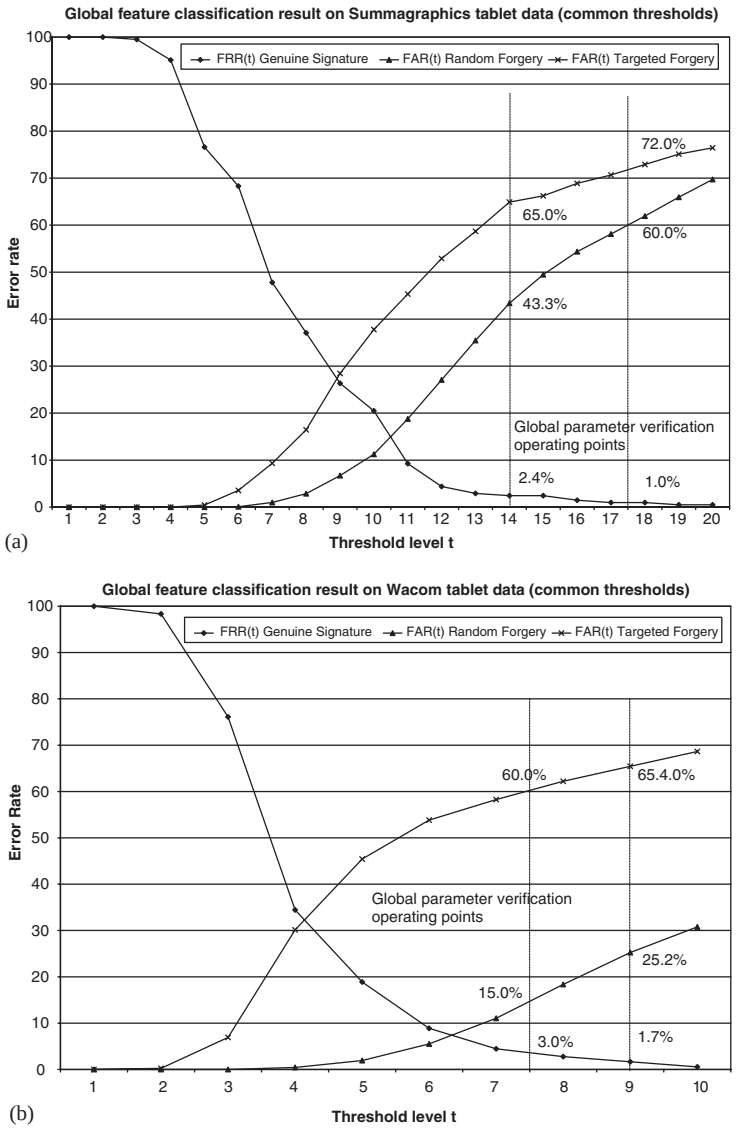

Fig. 13. Global parameter verification results signature data captured using (a) Summagraphics tablet and (b) Wacom Intuos tablet and wireless pen.

equal error rate (EER) increases towards 10%, due to the much less accurately estimated stability information and as a result the algorithm degenerates to one without stability weighting.

It can be seen from the error trade-off curves that, without SDG models, the EER is about 10% for detecting targeted and skilled forgery signatures, while the EER under global parameter tests is above 30%; with the addition of SDG model verification, the EER is reduced to about 5%; and with the introduction of stroke-segmentation and model refinement, it is further reduced to about 4% (Fig. 14). The EER on random forgery input is close to 0.2%, which is mostly due to the inclusion of a number of practiced names in DB1. This error rates are consistent with the figures given in a recent survey paper by Plamondon and Srihari [3], which is between 2% and 5%. Examples of the classified genuine and skilled forgery signatures are shown in Fig. 15.

The error cases are mostly due to:

- unreliable statistics of local and global features, based on a few consecutively written, closely resembling reference signatures, resulting in false rejection of subsequent genuine input which exhibits larger variations;

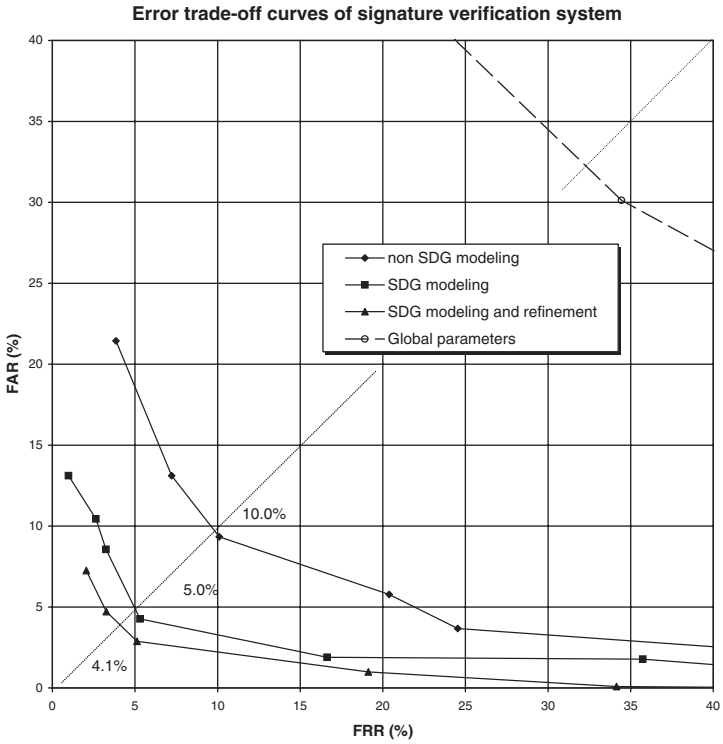

Fig. 14. The error trade-off curves of tests on targeted forgery signatures (DB1 and DB2), for the three cases of not using the SDG model, using the SDG model, and using the SDG model with stroke matching refinement. Five reference samples per signature class are used in training the signature models.

- excessive variation of identified stable components and strings in unseen variant signature styles, resulting in false rejection of genuine signatures;
- short and unstable reference signatures, resulting in forgery signatures being accepted.

Because of the lack of a common benchmark signature data set, it is difficult to compare signature verification algorithms in a quantitative manner. Therefore, a qualitative comparison is made to recent results in the literature. The proposed signature verification algorithm, although a matching-based technique, is in a sense similar to an HMM approach. It combines dynamic warping and statistical stability modeling about handwriting components, which conceptually corresponds to the HMM's Viterbi algorithm and the state and state-transition probability modeling. In the work by Dolfing et al., an HMM-based approach is investigated, and the reported EER is about 1.0–1.9% [10], better than that of the proposed algorithm. However, the number of training signatures used is much higher, with 15 training samples per class and a further five as a validation set. At the same time, short and unreliable signature enrollments, i.e. signatures taking less than 1.25 s to sign, are rejected to achieve the lower EER. In a recent publication, Jain et al. detailed a string-matching-based signature verification algorithm, and investigated the effectiveness of feature combinations. In their experiment, three to five reference samples are used in training, which is similar to the experiment setting in this paper. The best result is reported to be a false rejection rate of 2.8% and a corresponding false acceptance rate of 1.6%. Tests on both random and skilled forgery signatures are performed; however, the number of skilled forgery used in the tests is limited [35,7].

In the proposed algorithm, the improvement brought by the introduction of SDG models is significant, due to the identification and emphasis on the matchings of the stable handwriting components and component strings in a signature. The improvement by stroke segmentation refinement process is observed in combination with stability modeling, and its advantage is also evident. Because not all the segmentation errors can be identified automatically, the unidentified segmentation errors are labeled as style variations instead by the algorithm. The effectiveness of the refinement process can be improved if these errors can be correctly located, e.g. by supplying more representative reference signatures.

Fig. 15. Verification results showing the decision output for some genuine and targeted or skilled forgery signatures.

6. Further directions

The signature modeling technique presented can be extended, by implementing a strategy similar to the following, to support gradual reference model updating, in order to keep up with handwriting variations over time. By ranking the utilization of each SDG model in the acceptance tests, under regular usage, over a specified long period of time, a histogram of the utilization frequency of the models can be built. The lowest ranking model is likely to be phased out. New reference models will be constructed using recent input signatures that have been successfully accepted. However, the newly constructed models will not be directly used in verification but acts as pseudo-models for a further period of time, until it is proven that their ranks are consistently higher than the ones to be replaced. The optimal time

periods and other system update parameters are to be determined experimentally in practical situations.

7. Conclusion

An SDG-based stability modeling technique has been introduced in this paper. It is used to improve a stroke-based on-line signature verification system developed previously. The improvements include stability considerations in the verification score, signature segmentation verification, and signature SDG model building. The stability feature extraction algorithm will quantify how important or how consistent the segmentation points are. Style variations are explicitly allowed for by following all permissible paths within the SDGs, and errors in signature segmentation are eliminated or partially corrected by the stroke-match refinement process. These result in a more thorough utilization of available reference signatures. The DTW technique is an essential part of the proposed signature verification method. It operates on signature components and strings to extract component-level and string-level correspondence and stability information and calculates signature matching similarity accordingly. Although the handwriting motion-based signature segmentation technique is adopted here to generate the basis signature segmentation structure, the verification algorithm is not restricted to motion segmentation. Other segmentation techniques, such as segmenting the signature at perceptually important points [36], may also be applicable.

References

[1] R. Plamondon, G. Lorette, Automatic signature verification and writer identification: the state of the art, Pattern Recognition 22 (2) (1989) 107–131.

[2] F. Leclerc, R. Plamondon, Automatic signature verification: the state of the art—1989–1993, in: R. Plamondon (Ed.), Special Issue on Automatic Signature Verification, Int. J. Pattern Recognition Artif. Intell. 8(3) (1994) 3–19.

[3] R. Plamondon, S.N. Srihari, On-line and off-line handwriting recognition: a comprehensive survey, IEEE Trans. Pattern Anal. Mach. Intell. 14 (1) (2000) 3–19.

[4] M. Parizeau, R. Plamondon, A comparative analysis of regional correlation, dynamic time warping, and skeletal tree matching for signature verification, IEEE Trans. Pattern Anal. Mach. Intell. 12 (7) (1990) 710–718.

[5] Y. Sato, K. Kogure, Online signature verification based on shape, motion, and writing pressure, Proceedings of the Sixth International Conference on Pattern Recognition, Munich, 1982, pp. 823–826.

[6] V.S. Nalwa, Automatic on-line signature verification, Proc. IEEE 85 (2) (1997) 215–239.

[7] A.K. Jain, F.D. Griess, S.D. Connell, On-line signature verification, Pattern Recognition 35 (12) (2002) 2963–2972.

[8] M.J. Paulik, N. Mohankrishnan, 1-D, sequence decomposition based, autoregressive hidden Markov model for dynamic signature identification and verification, Midwest Symp. Circuits Systems 1 (1993) 138–141.

[9] L. Yang, B.K. Widjaja, R. Prasad, Application of hidden Markov models for signature verification, Pattern Recognition 28 (2) (1995) 161–170.

[10] J.G.A. Dolfing, E.H.L. Aarts, J.J.G.M. Van Oosterhout, On-line signature verification with Hidden Markov models, Proceedings of the 14th International Conference on Pattern Recognition, Brisbane, 1998, pp. 1309–1312.

[11] G. Rigoll, A. Kosmala, A systematic comparison between on-line and off-line methods for signature verification with hidden Markov models, Proceedings of the 14th International Conference on Pattern Recognition, Brisbane, Australia, August 16–20, 1998, pp. 1755–1757.

[12] J. Bromley, J.W. Bentz, L. Bottou, I. Guyon, Y. LeCun, C. Moore, E. Sackinger, R. Shah, Signature verification using a "siamese" time delay neural network, Int. J. Pattern Recognition Artif. Intell. 8 (3) (1994) 669–687.

[13] Quen-Zong Wu, Suh-Yin Lee, I-Chang Jou, On-line signature verification using LPC Cepstrum and neural network, IEEE Trans. Systems Man Cybernet. 27 (1) (1997) 148–153.

[14] Wan-Suck Lee, N. Mohankrishnan, M.J. Paulik, Improved segmentation through dynamic time warping for signature verification using a neural network classifier, Proceedings of the 1998 IEEE ICIP, Part 2 (of 3), Chicago, Illinois, USA, Oct 4–7, 1998, pp. 929–933.

[15] K. Huang, H. Yan, Identifying and verifying handwritten signature images utilizing neural networks, Proceedings of ICONIP'96, Hong Kong, September 1996, pp. 1400–1404.

[16] N.A. Murshed, R. Sabourin, F. Bortolozzi, A cognitive approach to off-line signature verification, Int. J. Pattern Recognition Artif. Intell. 11 (5) (1997) 801–825.

[17] Xuhong Xiao, G. Leedham, Signature verification using a modified Bayesian network, Pattern Recognition 35 (5) (2002) 983–995.

[18] K. Huang, H. Yan, Off-line signature verification using structural feature correspondence, Pattern Recognition 35 (11) (2002) 2467–2477.

[19] G. Dimauro, S. Impedovo, G. Pirlo, A new methodology for the measurement of local stability in dynamical signatures, Proceedings of IWFHR-IV, Taipei, 1994, pp. 135–144.

[20] V. Di Lecce, G. Dimauro, A. Guerriero, S. Impedovo, G. Pirlo, A. Salzo, L. Sarcinella, Selection of reference signatures for automatic signature verification, Proceedings of ICDAR'99, Fifth International Conference on Document Analysis and Recognition, Bangalore, India, September 20–22, 1999, pp. 597–600.

[21] G. Dimauro, S. Impedovo, R. Modugno, G. Pirlo, Analysis of stability in hand-written dynamic signatures, Proceedings of the Eighth International Workshop on Frontiers in Handwriting Recognition (IWFHR'02), Ontario, Canada, August 6–8, 2002, pp. 259–263.

[22] R. Plamondon, F.J. Maarse, An evaluation of motor models of handwriting, IEEE Trans. Systems Man Cybernet. 19 (5) (1989) 1060–1072.

[23] R. Plamondon, A model-based segmentation framework for computer processing of handwriting, Proceedings of the 11th International Conference on Pattern Recognition, The Hague, The Netherlands, 1992, pp. 303–307.

[24] R. Plamondon, P. Yergeau, J.J. Brault, A multi-level signature verification system, in: S. Impedovo, J.C. Simon (Eds.), From Pixels to Features III: Frontiers in Handwriting Recognition, Elsevier Science, New York, 1992, pp. 363–370.

[25] R. Plamondon, The design of an on-line signature verification system: from theory to practice, in: R. Plamondon (Ed.), Special Issue on Automatic Signature Verification, Int. J. Pattern Recognition Artif. Intell. 8(3) (1994) 795–811.
[26] P. Morasso, F.A. Mussa Ivaldi, Trajectory formation and handwriting: a computational model, Biol. Cybern. 45 (1982) 131–142.
[27] L.R.B. Schomaker, R. Plamondon, The relation between axial pen force and pen-point kinematics in handwriting, Biol. Cybern. 63 (1990) 277–289.
[28] K. Huang, H. Yan, On-line signature verification based on dynamic segmentation and global and local matching, Opt. Eng. 34 (12) (1995) 3480–3487.
[29] G. Dimauro, S. Impedovo, G. Pirlo, A signature verification system based on a dynamic segmentation technique, Proceedings of the Third International Workshop on Frontiers in Handwriting Recognition, Buffalo, USA, 1993, pp. 262–271.
[30] Taik H. Rhee, Sung J. Cho, Jin H. Kim, On-line signature verification using model-guided segmentation and discriminative feature selection for skilled forgeries, Proceedings of ICDAR'01, Sixth International Conference on Document Analysis and Recognition, Seattle, Washington, USA, September 10–13, 2001, pp. 645–649.
[31] G. Dimauro, S. Impedovo, G. Pirlo, A stroke-oriented approach to signature verification, in: S. Impedovo, J.C. Simon (Eds.), From Pixels to Features III: Frontiers in Handwriting Recognition, Elsevier Science, New York, 1992, pp. 371–384.
[32] G. Dimauro, S. Impedovo, G. Pirlo, Component-oriented algorithms for signature verification, Int. J. Pattern Recognition Artif. Intell. 8 (3) (1994) 771–793.
[33] K. Huang, H. Yan, Off-line signature verification based on geometric feature extraction and neural network classification, Pattern Recognition 30 (1) (1997) 9–17.
[34] K. Huang, H. Yan, Signature verification using fractal transformation, Proceedings of the 15th IAPR International Conference on Pattern Recognition, Barcelona, 2000, pp. 855–858.
[35] F.D. Griess, On-line signature verification, Masters Thesis MSU-CSE-00-15, Computer Sciences Department, Michigan State University, May 2000.
[36] J.-J. Brault, R. Plamondon, Segmenting handwritten signature at their perceptually important points, IEEE Trans. Pattern Anal. Mach. Intell. 15 (9) (1993) 953–957.

About the Author—KAI HUANG received his B.Sc. and B.E. degree in 1991 and 1993, respectively, from the University of Sydney. He is currently a Ph.D. candidate in the School of Electrical and Information Engineering at the same university. His research interests include pattern recognition, signal and image processing, and automatic handwritten signature verification.

About the Author—HONG YAN received a B.E. degree from Nanking Institute of Posts and Telecommunications in 1982, an M.S.E. degree from the University of Michigan in 1984, and a Ph.D. degree from Yale University in 1989, all in electrical engineering.
In 1982 and 1983 he worked on signal detection and estimation as a graduate student and research assistant at Tsinghua University. From 1986 to 1989 he was a research scientist at General Network Corporation, New Haven, CT, USA, where he worked on design and optimization of computer and telecommunications networks. He joined the University of Sydney in 1989 and became Professor of Imaging Science in the School of Electrical and Information Engineering in 1997. He is currently Professor of Computer Engineering at the City University of Hong Kong.

His research interests include bioinformatics, computer animation, signal and image processing, pattern recognition, neural and fuzzy algorithms. He is author or co-author of one book and over 200 refereed technical papers in these areas. Professor Yan is a fellow of the International Association for Pattern Recognition (IAPR), a fellow of the Institution of Engineers, Australia (IEAust), a senior member of the Institute of Electrical and Electronic Engineers (IEEE), and a member of the International Society for Optical Engineers (SPIE), the International Neural Network Society (INNS), and the International Society for Magnetic Resonance in Medicine (ISMRM).